

A vascular niche and a VEGF–Nrp1 loop regulate the initiation and stemness of skin tumours

Benjamin Beck¹, Gregory Driessens¹, Steven Goossens^{2,3}, Khalil Kass Youssef¹, Anna Kuchnio^{3,4}, Amélie Caauwe¹, Panagiota A. Sotiropoulou¹, Sonja Loges^{4,5,†}, Gaele Lapouge¹, Aurélie Candi¹, Guilhem Mascré¹, Benjamin Drogat¹, Sophie Dekoninck¹, Jody J. Haigh^{2,3}, Peter Carmeliet^{4,5} & Cédric Blanpain^{1,6}

Angiogenesis is critical during tumour initiation and malignant progression¹. Different strategies aimed at blocking vascular endothelial growth factor (VEGF) and its receptors have been developed to inhibit angiogenesis in cancer patients². It has become increasingly clear that in addition to its effect on angiogenesis, other mechanisms including a direct effect of VEGF on tumour cells may account for the efficiency of VEGF-blockade therapies³. Cancer stem cells (CSCs) have been described in various cancers including squamous tumours of the skin^{4,5}. Here we use a mouse model of skin tumours to investigate the impact of the vascular niche and VEGF signalling on controlling the stemness (the ability to self-renew and differentiate) of squamous skin tumours during the early stages of tumour progression. We show that CSCs of skin papillomas are localized in a perivascular niche, in the immediate vicinity of endothelial cells. Furthermore, blocking VEGFR2 caused tumour regression not only by decreasing the microvascular density, but also by reducing CSC pool size and impairing CSC renewal properties. Conditional deletion of *Vegfa* in tumour epithelial cells caused tumours to regress, whereas VEGF overexpression by tumour epithelial cells accelerated tumour growth. In addition to its well-known effect on angiogenesis, VEGF affected skin tumour growth by promoting cancer stemness and symmetric CSC division, leading to CSC expansion. Moreover, deletion of neuropilin-1 (*Nrp1*), a VEGF co-receptor expressed in cutaneous CSCs, blocked VEGF's ability to promote cancer stemness and renewal. Our results identify a dual role for tumour-cell-derived VEGF in promoting cancer stemness: by stimulating angiogenesis in a paracrine manner, VEGF creates a perivascular niche for CSCs, and by directly affecting CSCs through *Nrp1* in an autocrine loop, VEGF stimulates cancer stemness and renewal. Finally, deletion of *Nrp1* in normal epidermis prevents skin tumour initiation. These results may have important implications for the prevention and treatment of skin cancers.

Skin squamous cell carcinoma is the second most frequent skin cancer in humans and affects about 500,000 new patients per year worldwide⁶. Mouse models for skin squamous tumours are almost identical to human skin cancers and thus offer an ideal model to study cancer initiation and growth⁷. The most extensively used mouse cancer model relies on chemically (9,10-dimethyl-1,2-benzanthracene (DMBA) and 12-*O*-tetradecanoyl phorbol-13-acetate (TPA)) induced skin carcinogenesis protocol⁸. In this model, the number of papillomas is a measure of tumour initiation, whereas the growth rate is an indicator of tumour promotion. Recently, CD34-expressing tumour epithelial cells (TECs) isolated from DMBA/TPA-induced skin tumours were identified as CSCs, based on their increased clonogenic potential and ability to form secondary tumours upon transplantation into immunodeficient mice⁵. It has been suggested that the tumour microenvironment, in particular

the vascular niche, can influence CSC function in brain tumours⁹, but whether CD34⁺ CSCs are located in a vascular niche and whether these vessels regulate CSC function and stemness remain unknown.

To assess whether CSCs of skin papillomas reside in a perivascular niche, we performed triple immunostaining for cutaneous CSC markers (see below) (CD34, Hmga2 and Krt13), TEC markers (K5 and K14) and endothelial cell markers (endoglin and CD31). Papillomas are well organized and differentiated tumours containing one or two layers of proliferating basal-like cells, expressing K5 and β 4-integrin, which give rise to several layers of differentiated tumour cells expressing K1/K10 and loricrin (Supplementary Fig. 1). As expected, skin CSCs co-expressed cutaneous CSC and TEC markers, but did not express endothelial cell markers and can thus be reliably distinguished from vascular endothelial cells (Fig. 1a, b and Supplementary Fig. 2). Interestingly, most CSCs were detected in close proximity to endothelial cells (within 30 μ m), whereas the more differentiated tumour cells were located more distantly from endothelial cells (Fig. 1a, b and Supplementary Fig. 2), indicating that CSCs of skin papilloma may reside in a vascular niche, similarly to what has been described for haematopoietic stem cells^{10,11} and CSCs in brain tumours⁹.

To determine the role of the vascular microenvironment in regulating the stemness of skin tumours, we used an antibody-based strategy to inhibit angiogenesis by blocking VEGFR2 signalling in endothelial cells (Fig. 1c). In skin papillomas, VEGFR2 is almost exclusively expressed by endothelial cells and is not detectable in TECs (Fig. 1d, e and Supplementary Fig. 3). Administration of a blocking antibody against VEGFR2 (DC101)—a powerful inhibitor of tumour angiogenesis¹²—to mice with established skin papillomas resulted in tumour regression and a significant decrease in endothelial cell proliferation and tumour microvascular density (Fig. 1f–h and Supplementary Fig. 4), consistent with previous anti-angiogenic reports of DC101 in human squamous cell carcinoma xenografts¹³. Notably, DC101 also reduced the proportion of CD34⁺ CSCs, as determined by immunofluorescence (K5⁺CD34⁺) and FACS analysis (Epcam⁺CD34⁺), and the decrease in tumour microvascular density closely correlated with the decrease in the CD34⁺ CSC pool size (Fig. 1i, j and Supplementary Fig. 5). This decrease in CD34⁺ TECs was not due to an increase in CSC apoptosis, but rather to a reduction in CSC proliferation (Fig. 1k, l and Supplementary Fig. 6). We therefore explored whether VEGF might also affect CSCs directly using various genetic gain- and loss-of-function approaches.

Deletion of *Vegfa* in epidermal cells prevents squamous skin tumour development^{14,15}, whereas transgenic overexpression of VEGF increases the number and accelerates the growth of papillomas after DMBA/TPA treatment^{16,17}. Thus, VEGF is already known to regulate skin tumour initiation, but its role in regulating cancer stemness, and thereby skin tumour progression, remains unknown. Notably, quantitative

¹IRIBHM, Université Libre de Bruxelles, 808 route de Lennik, 1070 Brussels, Belgium. ²Vascular Cell Biology Unit, VIB Department for Molecular Biomedical Research, 9052 Ghent, Belgium. ³UGent Department for Molecular Biomedical Research, 9052 Ghent, Belgium. ⁴Laboratory of Angiogenesis and Neurovascular Link, Vesalius Research Center, VIB, 3000 Leuven, Belgium. ⁵Laboratory of Angiogenesis and Neurovascular Link, Vesalius Research Center, K.U. Leuven, 3000 Leuven, Belgium. ⁶Welbio, IRIBHM, Université Libre de Bruxelles, 808 route de Lennik, 1070 Brussels, Belgium. [†]Present address: Universitätsklinikum Hamburg-Eppendorf, II, Medical Clinic & Institute of Tumor Biology, Hamburg 20246, Germany.

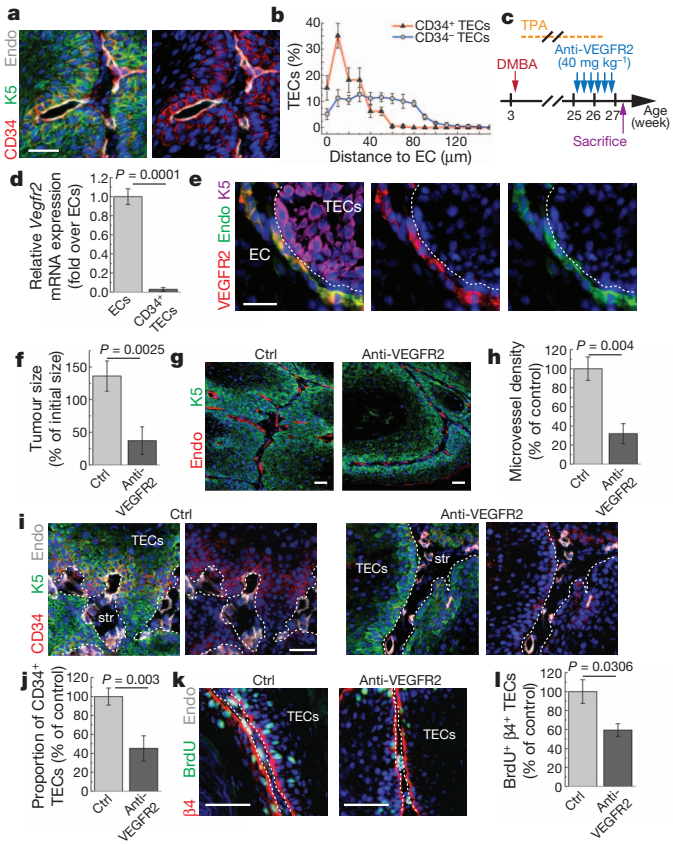


Figure 1 | A perivascular niche regulates cancer stemness in skin papilloma. **a**, Immunostaining for CD34, keratin 5 (K5) and endoglin (Endo). Hoechst nuclear staining is represented in blue. **b**, Distribution of the CD34⁺ and CD34⁻ TECs relative to the distance to endothelial cells; *n* = 8 papillomas. EC, endothelial cell. **c**, Protocol of DMBA/TPA and of anti-VEGFR2 blocking antibody administration. **d**, qRT-PCR analysis of *Vegfr2* mRNA expression in FACS-isolated tumour endothelial cells and CD34⁺ TECs; *n* = 6 papillomas. **e**, Immunostaining for VEGFR2, endoglin and K5 in a papilloma shows that VEGFR2 is only expressed by endothelial cells. **f**, Tumour size after 2 weeks of anti-VEGFR2 treatment; *n* = 36 papillomas. **g**, Immunostaining for endoglin and K5 in papillomas treated with control IgG or anti-VEGFR2. **h**, Microvessel density; *n* = 12 tumours. **i**, Immunostaining for CD34, K5 and endoglin. str, tumour stroma. **j**, FACS quantification of CD34⁺ TECs. **k**, Immunostaining for β4 integrin (β4), BrdU and endoglin. **l**, Proliferation of TECs as measured by BrdU incorporation in β4⁺ TECs after treatment with control or anti-VEGFR2 antibodies for 2 weeks; *n* = 12 papillomas. All scale bars represent 50 µm; all error bars represent s.e.m.

polymerase chain reaction with reverse transcription (qRT-PCR) showed that *Vegfa* mRNA is expressed at higher levels in CD34⁺ CSCs than in normal epidermal cells or CD34⁻ TECs (Fig. 2a). To explore whether VEGF expression by TECs regulates the stemness properties of cutaneous CSCs and is required to sustain tumour growth, we deleted *Vegfa* in TECs by administering tamoxifen to *K14CreER:VEGF^{f/f}* mice¹⁸ once they had established skin papillomas (Fig. 2b, c). As soon as 1 week after tamoxifen administration, most of the papillomas had shrunk by 60% and 2 weeks after, most of the papillomas had completely disappeared (Fig. 2d). As expected, tumour regression was associated with a decrease in endothelial cell proliferation and microvascular density (Fig. 2e, f and Supplementary Fig. 7). However, the magnitude of the antitumour effect suggested that inhibition of angiogenesis alone could not fully explain the complete disappearance of the established tumours. Indeed, the loss of VEGF in TECs also resulted in a marked reduction in the proportion of CD34⁺ TECs (Fig. 2g, h), and a strong decrease in basal cell proliferation (Fig. 2i, j), indicating that VEGF secretion by TECs has an impact on cutaneous CSCs as well.

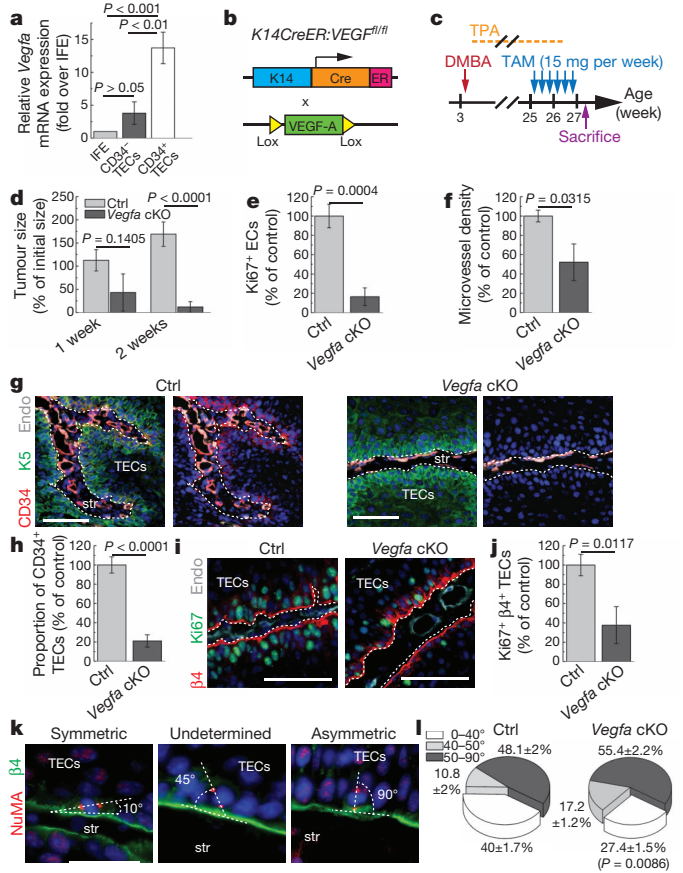


Figure 2 | VEGF expression by tumour cells is required for the maintenance of cutaneous cancer stem cells. **a**, qRT-PCR for *Vegfa* in normal interfollicular keratinocytes (IFE), CD34⁺ TECs and CD34⁻ TECs; *n* = 6 papillomas per condition. **b**, Genetic strategy used to study the role of VEGF-A expression by TECs. **c**, Protocol of DMBA/TPA and tamoxifen (TAM) administration (15 mg per week) in control and *Vegfa* conditional knockout (cKO) mice; *n* = 30. **d**, Tumour size 1 and 2 weeks after the beginning of tamoxifen administration (15 mg per week) in control and *Vegfa* conditional knockout (cKO) mice; *n* = 6 tumours. **e**, Proliferation of endothelial cells as determined by the proportion of Ki67⁺/endoglin⁺ endothelial cells 2 weeks after tamoxifen administration; *n* = 6 tumours. **f**, Microvessel density 1 week after tamoxifen administration; *n* = 12 tumours. **g**, Immunostaining for CD34, K5 and endoglin in a representative papilloma from mice of each genotype. **h**, FACS quantification of CD34⁺ TECs after tamoxifen administration; *n* = 6 papillomas. **i**, Immunostaining for β4 integrin (β4), endoglin and Ki67 in papillomas 1 week after tamoxifen administration. **j**, TEC proliferation as measured by the proportion of Ki67⁺/β4⁺ TECs in papillomas from each genotype 2 weeks after tamoxifen administration; *n* = 12 tumours. **k**, Immunostaining for β4 integrin (β4, green) and NuMa (red) in papillomas. **l**, Quantification of the division planes as measured by the angle between the centrosomal axis (NuMa) and the basal membrane (β4-integrin) in control and *Vegfa* cKO papillomas; *n* = 162 (*vegfa* cKO) and 258 (Ctrl) cells. For each panel showing immunostaining, Hoechst nuclear staining is represented in blue. All scale bars represent 50 µm; all error bars represent s.e.m.

This hypothesis was further underscored by analysis of symmetric versus asymmetric cell division of the CSCs. The orientation of the mitotic spindle controls the balance between epidermal progenitor self-renewal (symmetric cell division) and differentiation (asymmetric cell division) during embryonic development^{19–21}. Analysis of the orientation of mitotic spindle in TECs revealed that approximately 40% of the mitosis events during tumour growth were symmetric in nature. Interestingly, deletion of *Vegfa* in TECs led to a significant decrease in the proportion of symmetric self-renewing cell divisions (Fig. 2k, l). Loss of VEGF also resulted in a decrease in the number of layers of differentiated TECs, but no significant increase in apoptosis was observed (Supplementary Fig. 8). Thus, autocrine VEGF expression by TECs seems to be critical for the proliferation and renewal of cutaneous CSCs.

To establish further the critical autocrine role of VEGF, we also assessed whether increased VEGF production by TECs would increase CSC renewal. We therefore conditionally overexpressed VEGF specifically in TECs by administering tamoxifen to *K14CreER:Rosa26-VEGF-164* mice²², after they had already formed skin papillomas (Fig. 3a, b). Tamoxifen administration enhanced VEGF expression by TECs in *K14CreER:Rosa26-VEGF-164* mice, and resulted in accelerated tumour growth. As expected, this tumour-promoting effect of VEGF was accompanied by a strong increase in endothelial cell

proliferation and microvascular density (Fig. 3c, d and Supplementary Fig. 9). VEGF overexpression in TECs also caused a major expansion of the CD34⁺ CSC population, increased the proliferation of CD34⁺ CSCs, and the proportion of symmetric CSC division (Fig. 3e–i and Supplementary Fig. 10), altogether expanding the CD34⁺ CSC pool. Moreover, even though VEGF overexpression did not completely abrogate tumour cell differentiation, it did significantly delay tumour cell differentiation *in vitro* and *in vivo* (Supplementary Figs 10 and 14). Altogether, increased VEGF production by TECs enhanced tumour growth, not only by stimulating angiogenesis (and the formation of a vascular niche for CSCs) but also by promoting CSC renewal.

To underscore further the notion that VEGF altered the stemness properties of CD34⁺ CSCs and to determine the molecular mechanisms of how VEGF promotes the renewal of CD34⁺ CSCs, we transcriptionally profiled control and VEGF-overexpressing, FACS-isolated, CD34⁺ CSCs to determine any possible 'VEGF signature'. VEGF upregulated approximately 20% of the genes preferentially expressed by CD34⁺ CSCs as compared to CD34⁻ TECs (CD34⁺ signature), including genes known to regulate stemness (for example, *Sox2*, *Hmg2*), proliferation (*Ccnd1*, *Ccng1*) and the interaction of tumour cells with their microenvironment (*Colla1*, *Col3a1*), as well as genes known to be expressed in squamous cell carcinoma (*Krt13*, *Ano1*) (Fig. 3j, k, Supplementary Table 1 and Supplementary Fig. 11). Using qRT-PCR, FACS and immunostaining, we confirmed that around 50% of these genes were upregulated by VEGF (Fig. 3k–n and Supplementary Fig. 11). Thus, VEGF altered the transcriptional signature of CD34⁺ CSCs in a manner that would be expected to promote cancer stemness. Consistent herewith, transplantation of a limiting dilution of CD34⁺ TECs isolated from VEGF-overexpressing mice into immunodeficient mice increased the number of grafts with tumours compared to control CD34⁺ CSCs, whereas the opposite phenotype was observed when CD34⁺ VEGF-deficient CSCs were grafted (Supplementary Fig. 12). Thus, VEGF qualitatively altered the stemness properties of CSCs.

It has been shown recently that deletion of VEGFR1 (*flt1*) in epidermal cells delays the appearance of skin papilloma in *K5-Sos* transgenic mice¹⁴, indicating that VEGF signalling in keratinocytes can directly regulate the initiation of these skin tumours. To explore whether VEGF signalling could affect tumour progression by directly regulating cutaneous CSC properties, we sought to design an experimental strategy to impair VEGF signalling in TECs. We first analysed which of the VEGF receptors were expressed in CSCs from skin papillomas. qRT-PCR and immunostaining showed that neuropilin 1 (*Nrp1*) was expressed at the highest level by CD34⁺ CSCs (Fig. 4a and Supplementary Fig. 13). Besides its well-known role as co-receptor of the VEGF receptors in endothelial cells, NRP1 is also expressed in various human carcinoma cell lines and primary tumours^{23,24}. Furthermore, overexpression of *Nrp1* promotes the growth of cancer cell lines whereas anti-*Nrp1* blocking antibodies can inhibit tumour growth²⁵. However, it remains unclear whether *Nrp1* can control tumour initiation and stimulate tumour progression by promoting VEGF receptor signalling in endothelial cells or, additionally, by directly regulating VEGF signalling in TECs as previously suggested²³.

To explore the role of *Nrp1* in skin tumorigenesis, we performed, as a first step, a constitutive conditional deletion of *Nrp1* in the epidermis (*K14-Cre:Nrp1^{fl/fl}* mice, Fig. 4b). Mice lacking *Nrp1* in their epidermis are viable, develop normally and have normal skin (Supplementary Fig. 13). Chemical skin carcinogenesis was then initiated in *Nrp1*-deficient mice and their respective littermate controls. After DMBA/TPA treatment, 100% of the control mice developed skin papilloma after 25 weeks of TPA treatment, whereas, notably, mice lacking *Nrp1* in their epidermis did not develop any papilloma at this time point (Fig. 4c, d). These results indicate that *Nrp1* expression in epidermal cells is critical for skin tumour initiation.

To assess whether *Nrp1* might directly regulate cutaneous tumour stemness, independently of an effect on the vascular niche, we

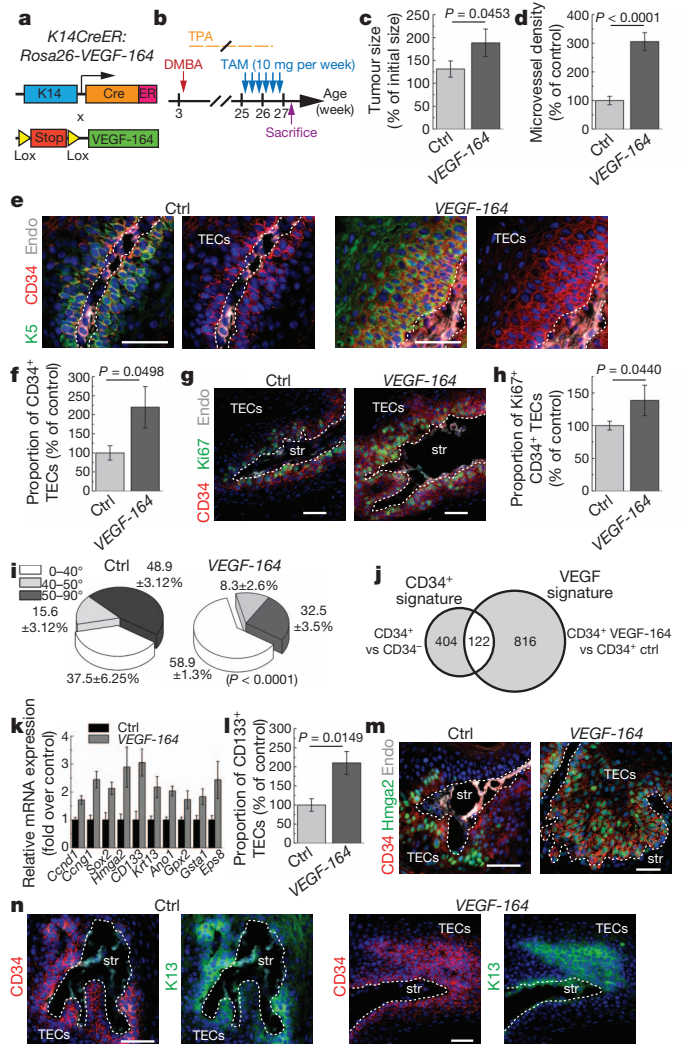


Figure 3 | Increased VEGF expression promotes cutaneous cancer-stem-cell expansion. **a**, Genetic strategy used to study the consequences of VEGF-A overexpression in TECs. **b**, Protocol of DMBA/TPA and tamoxifen administration. **c**, Tumour size 2 weeks after the first tamoxifen administration (10 mg per week); $n = 40$ tumours. **d**, Microvessel density 2 weeks after tamoxifen administration; $n = 15$ tumours. **e**, Immunostaining for K5, CD34 and endoglin. **f**, FACS quantification of the proportion of CD34⁺ TECs 2 weeks after tamoxifen administration. **g**, **h**, Immunostaining and quantification of Ki67⁺ and CD34⁺ TECs in control and VEGF-164 overexpressing papillomas; $n = 10$ tumours. **i**, Quantification of the division planes in control and VEGF-164 overexpressing papillomas; $n = 348$ (VEGF-164) and 192 (Ctrl) cells 2 weeks after tamoxifen administration. **j**, Venn diagram from microarray comparing CD34⁺ versus CD34⁻ TECs (CD34 signature) and control versus VEGF-164 CD34⁺ TECs (VEGF signature). **k**, mRNA expression of ten genes of the CD34 signature upregulated by VEGF-164 3 weeks after tamoxifen administration; $n = 3$ tumours. **l**, FACS quantification of the proportion of CD133⁺ TECs after VEGF-164 overexpression; $n = 6$ tumours. **m**, **n**, Immunostaining for CD34 and keratin 13 (K13) or Hmg2 in papillomas 2 weeks after tamoxifen administration. Hoechst nuclear staining is represented in blue; all scale bars represent 50 μm ; all error bars represent s.e.m.

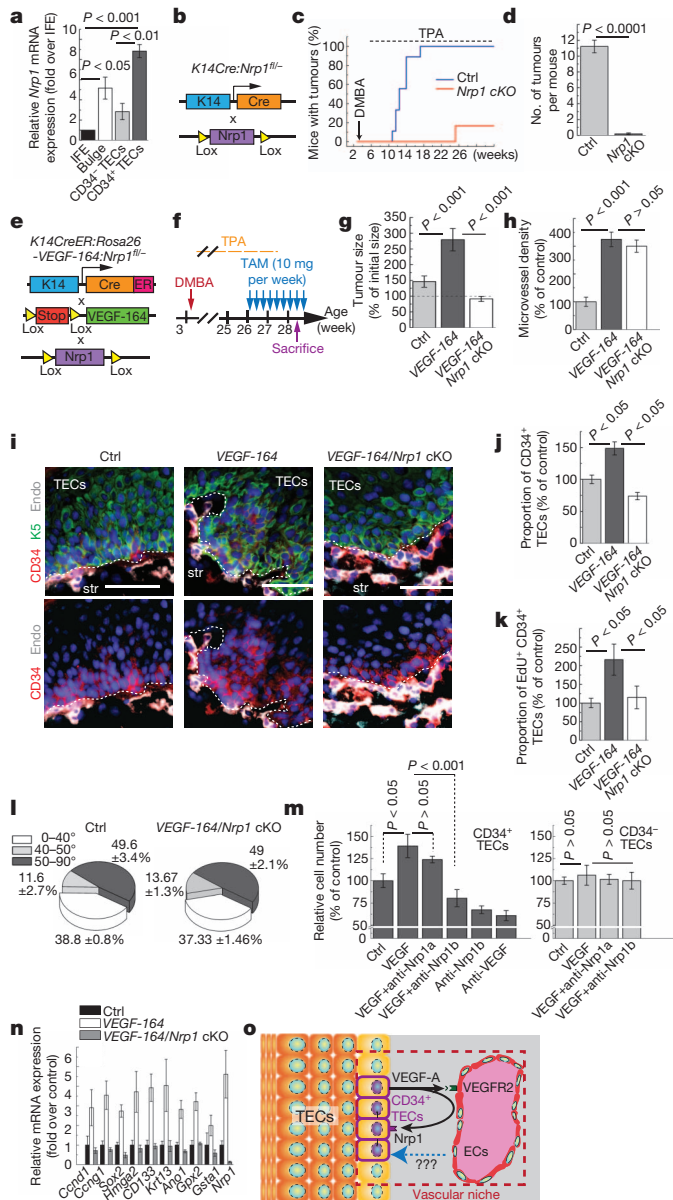


Figure 4 | *Nrp1* is required for squamous tumour initiation and regulates stemness of cutaneous cancer cells. **a**, qRT-PCR for *Nrp1* in normal interfollicular keratinocytes (IFE), $CD34^+$ hair follicle bulge stem cells, $CD34^-$ TECs and $CD34^+$ TECs; $n = 3$ tumours. **b**, Genetic strategy used to study the cell-autonomous role of *Nrp1* in skin tumour initiation (*K14Cre:Nrp1^{fl/fl}*). **c**, Percentage of control and *Nrp1* cKO mice presenting skin tumours. **d**, Average number of tumours per mouse 40 weeks after tumour initiation; Ctrl, $n = 9$; *Nrp1* cKO, $n = 11$ mice. **e**, Genetic strategy used to study the role of VEGF-164 and *Nrp1* in pre-established skin tumour. **f**, Protocol of DMBA/TPA and tamoxifen administration. **g**, Tumour size ($n = 30$ tumours) 3 weeks after tamoxifen administration. **h**, Microvessel density ($n = 15$ tumours) 3 weeks after tamoxifen administration. **i**, Immunostaining for K5, CD34 and endoglin. **j**, FACS quantification of the proportion of $CD34^+$ TECs 3 weeks after tamoxifen administration ($n = 9$ papillomas). **k**, Quantification of the proportion of $Edu^+ CD34^+$ TECs ($n = 9$ tumours) 3 weeks after tamoxifen administration in control, VEGF-overexpressing and VEGF-overexpressing *Nrp1*-deficient TECs. **l**, Quantification of the division planes in control and VEGF-164-overexpressing, *Nrp1*-deficient papillomas 3 weeks after tamoxifen administration; $n = 274$ for VEGF-164/*Nrp1^{fl/fl}* and $n = 224$ for control mice. **m**, Cell growth of FACS-isolated $CD34^+$ and $CD34^-$ TECs after 1 week of *in vitro* culture and treated with indicated molecules; $n = 9$ replicates. **n**, mRNA expression of 10 genes of the $CD34$ signature upregulated by VEGF, from control, VEGF-164 and VEGF-164/*Nrp1* cKO papillomas 3 weeks after tamoxifen administration; $n = 3$ tumours. **o**, Model of the dual role of VEGF in regulating cutaneous cancer stemness. Hoechst nuclear staining is represented in blue. All scale bars represent 50 μ m; all error bars represent s.e.m.

simultaneously deleted *Nrp1* and overexpressed VEGF selectively in TECs (Fig. 4e, f). Compared to VEGF overexpression in *Nrp1^{fl/fl}* cells or VEGF overexpression in wild-type cells, VEGF overexpression in *Nrp1^{fl/fl}* TECs no longer accelerated tumour growth (Fig. 4g). This inefficiency of VEGF was not due to an unresponsiveness of endothelial cells to paracrine VEGF, as VEGF overexpression by *Nrp1*-deficient TECs still increased tumour angiogenesis (Fig. 4h and Supplementary Fig. 14). However, by contrast, deletion of *Nrp1* in VEGF-overexpressing TECs abrogated the ability of VEGF to stimulate tumour cell proliferation, symmetric cell division and expansion of the $CD34^+$ CSC pool (Fig. 4i-l), indicating that *Nrp1*, in a cell-autonomous manner, mediated the response of CSCs to autocrine VEGF.

To investigate this molecular mechanism further, we cultured FACS-isolated $CD34^+$ and $CD34^-$ TECs *in vitro* and exposed them to VEGF, in the presence or not of anti-*Nrp1* blocking antibodies²⁵. VEGF stimulated the proliferation of $CD34^+$ but not $CD34^-$ TECs, and this effect was suppressed by an anti-*Nrp1* antibody that blocks its binding to VEGF, demonstrating that *Nrp1* cell-autonomously mediated the effect of VEGF on $CD34^+$ CSC proliferation. This effect was specific for VEGF-*Nrp1*, as an anti-*Nrp1* antibody that blocks the *Nrp1*-semaphorin interaction was ineffective (Fig. 4m). Comparative qRT-PCR analysis of FACS-isolated $CD34^+$ CSCs expressing or lacking *Nrp1* showed that *Nrp1* was required for the upregulation of most stemness and proliferation genes in response to VEGF (Fig. 4n and Supplementary Fig. 15). Thus, autocrine production of VEGF and *Nrp1* expression by the TECs regulates the stemness of cutaneous tumours and the expansion of the CSC pool, which, together with the pro-angiogenic activity of VEGF, contribute to enhanced tumour growth.

Our results indicate that VEGF has a dual role in the initial stage of skin tumour promotion. First, VEGF signalling through VEGFR2 in endothelial cells is critical to sustain angiogenesis and to create a vascular niche for CSCs. Whether endothelial cells in the perivascular niche produce angiocrine signals to foster stemness remains to be determined. Second, VEGF also acts directly on epidermal cells and cutaneous CSCs through a cell-autonomous mechanism depending on *Nrp1*, and hereby also increases the stemness and renewal potential of CSCs; this autocrine loop contributes to skin tumour initiation and CSC expansion in early skin tumours (Fig. 4o). Such a dual role for VEGF in promoting stemness of CSCs *in vivo* by regulating both the vascular microenvironment and intrinsic stem-cell properties has important implications for the prevention and treatment of epithelial cancers.

METHODS SUMMARY

Tumour formation was performed by DMBA/TPA administration. Inhibition of VEGFR2 was performed by administrating anti-VEGFR2 antibodies to mice bearing papillomas. Gain and loss of VEGF and *Nrp1* function in skin tumours was performed by administrating tamoxifen to *K14CreER:VEGF^{fl/fl}*, *K14CreER:RosaVEGF-164* and *K14CreER:RosaVEGF-164:Nrp1^{fl/fl}* mice bearing skin tumours. The measurement of tumour size, cell proliferation, plane of cell division, apoptosis, differentiation and frequency of cancer stem cells were performed as described in Methods.

After enzymatic digestion of the tumours, $CD34^+$ TECs were isolated or quantified by FACS using a combination of monoclonal antibodies. Secondary tumour assays were performed by transplanting $CD34^+$ TECs into immunodeficient mice treated with tamoxifen. mRNA expression was quantified by Affymetrix Mouse Genome 430 2.0 Array or real-time RT-PCR using the primers and protocol indicated in Methods. FACS-isolated $CD34^+$ and $CD34^-$ TECs were cultured *in vitro* and treated with VEGF, anti-VEGF and anti-*Nrp1* blocking antibodies. For further details see Supplementary Methods.

Full Methods and any associated references are available in the online version of the paper at www.nature.com/nature.

Received 17 November 2010; accepted 24 August 2011.

1. Kerbel, R. S. Tumour angiogenesis. *N. Engl. J. Med.* **358**, 2039–2049 (2008).
2. Ferrara, N., Mass, R. D., Campa, C. & Kim, R. Targeting VEGF-A to treat cancer and age-related macular degeneration. *Annu. Rev. Med.* **58**, 491–504 (2007).

3. Ellis, L. M. & Hicklin, D. J. VEGF-targeted therapy: mechanisms of anti-tumour activity. *Nature Rev. Cancer* **8**, 579–591 (2008).
4. Lobo, N. A., Shimono, Y., Qian, D. & Clarke, M. F. The biology of cancer stem cells. *Annu. Rev. Cell Dev. Biol.* **23**, 675–699 (2007).
5. Malanchi, I. *et al.* Cutaneous cancer stem cell maintenance is dependent on β -catenin signalling. *Nature* **452**, 650–653 (2008).
6. Alam, M. & Ratner, D. Cutaneous squamous-cell carcinoma. *N. Engl. J. Med.* **344**, 975–983 (2001).
7. Perez-Losada, J. & Balmain, A. Stem-cell hierarchy in skin cancer. *Nature Rev. Cancer* **3**, 434–443 (2003).
8. Kemp, C. J. Multistep skin cancer in mice as a model to study the evolution of cancer cells. *Semin. Cancer Biol.* **15**, 460–473 (2005).
9. Calabrese, C. *et al.* A perivascular niche for brain tumor stem cells. *Cancer Cell* **11**, 69–82 (2007).
10. Butler, J. M., Kobayashi, H. & Rafii, S. Instructive role of the vascular niche in promoting tumour growth and tissue repair by angiocrine factors. *Nature Rev. Cancer* **10**, 138–146 (2010).
11. Kiel, M. J. & Morrison, S. J. Maintaining hematopoietic stem cells in the vascular niche. *Immunity* **25**, 862–864 (2006).
12. Witte, L. *et al.* Monoclonal antibodies targeting the VEGF receptor-2 (Flk1/KDR) as an anti-angiogenic therapeutic strategy. *Cancer Metastasis Rev.* **17**, 155–161 (1998).
13. Miller, D. W. *et al.* Rapid vessel regression, protease inhibition, and stromal normalization upon short-term vascular endothelial growth factor receptor 2 inhibition in skin carcinoma heterotransplants. *Am. J. Pathol.* **167**, 1389–1403 (2005).
14. Lichtenberger, B. M. *et al.* Autocrine VEGF signaling synergizes with EGFR in tumor cells to promote epithelial cancer development. *Cell* **140**, 268–279 (2010).
15. Rossiter, H. *et al.* Loss of vascular endothelial growth factor A activity in murine epidermal keratinocytes delays wound healing and inhibits tumor formation. *Cancer Res.* **64**, 3508–3516 (2004).
16. Hirakawa, S. *et al.* VEGF-A induces tumor and sentinel lymph node lymphangiogenesis and promotes lymphatic metastasis. *J. Exp. Med.* **201**, 1089–1099 (2005).
17. Larcher, F., Murillas, R., Bolontrade, M., Conti, C. J. & Jorcano, J. L. VEGF/VPF overexpression in skin of transgenic mice induces angiogenesis, vascular hyperpermeability and accelerated tumor development. *Oncogene* **17**, 303–311 (1998).
18. Gerber, H. P. *et al.* VEGF is required for growth and survival in neonatal mice. *Development* **126**, 1149–1159 (1999).
19. Lechler, T. & Fuchs, E. Asymmetric cell divisions promote stratification and differentiation of mammalian skin. *Nature* **437**, 275–280 (2005).
20. Poulson, N. D. & Lechler, T. Robust control of mitotic spindle orientation in the developing epidermis. *J. Cell Biol.* **191**, 915–922 (2010).
21. Williams, S. E., Beronja, S., Pasolli, H. A. & Fuchs, E. Asymmetric cell divisions promote Notch-dependent epidermal differentiation. *Nature* **470**, 353–358 (2011).
22. Maes, C. *et al.* Increased skeletal VEGF enhances β -catenin activity and results in excessively ossified bones. *EMBO J.* **29**, 424–441 (2010).
23. Soker, S., Takashima, S., Miao, H. Q., Neufeld, G. & Klagsbrun, M. Neuropilin-1 is expressed by endothelial and tumor cells as an isoform-specific receptor for vascular endothelial growth factor. *Cell* **92**, 735–745 (1998).
24. Staton, C. A., Kumar, I., Reed, M. W. & Brown, N. J. Neuropilins in physiological and pathological angiogenesis. *J. Pathol.* **212**, 237–248 (2007).
25. Pan, Q. *et al.* Blocking neuropilin-1 function has an additive effect with anti-VEGF to inhibit tumor growth. *Cancer Cell* **11**, 53–67 (2007).

Supplementary Information is linked to the online version of the paper at www.nature.com/nature.

Acknowledgements We thank Genetech for providing blocking anti-Nrp1 antibodies and H. Fujisawa, N. Ferrara and A. Nagy for providing the *Nrp1^{fl/fl}*, *Vegf^{fl/fl}* and *ROSA26-VEGF-164* mice, respectively. C.B. is an investigator of Welbio. C.B. and P.A.S. are chercheur qualifié and B.B. is a chargé de recherche of the FRS/FNRS; Am.C. and G.M. are research fellows of the FRS/FRIA. G.D. is supported by the Brussels Region, B.D. and K.K.Y. by TELEVE and S.G. is a postdoctoral fellow of the Basic Science Research Foundation-Flanders (FWO). S.L. is funded by the Max-Eder group leader program of the Deutsche Krebshilfe, by the Hamburger Krebsgesellschaft and by the Roggenbuck Stiftung. P.C. is funded by Long-term structural Methusalem funding by the Flemish Government. This work was supported by the FNRS, the program d'excellence CIBLES of the Wallonia Region, a research grant from the Fondation Contre le Cancer, the ULB foundation and the fond Gaston Ithier, a starting grant of the European Research Council (ERC) and the EMBO Young Investigator Program.

Author Contributions C.B., B.B., G.D., S.G., K.K.Y., P.C. and J.J.H. designed the experiments and performed data analysis. B.B., G.D., S.G., K.K.Y., G.L., S.L. and A.K. performed most of the experiments; P.A.S., Au.C., G.M. and B.D. contributed to mice treatment; S.D. and Am.C. provided technical support. C.B. and B.B. wrote the manuscript.

Author Information Microarray data have been deposited in the GEO database under accession number GSE31465. Reprints and permissions information is available at www.nature.com/reprints. The authors declare no competing financial interests. Readers are welcome to comment on the online version of this article at www.nature.com/nature. Correspondence and requests for materials should be addressed to C.B. (cedric.blanpain@ulb.ac.be).

METHODS

Mice. FVB/N mice were obtained from Charles River Laboratories. *K14Cre* (ref. 26) and *K14CreER* (ref. 27) transgenic mice were provided by E. Fuchs. *K14CreER* and *K14Cre* mice were mated with *Rosa26-VEGF-164*, *Vegf^{fl/fl}* (ref. 28) and *Nrp1^{fl/-}* (ref. 29) mice. Mouse colonies were maintained in a certified animal facility in accordance with European guidelines. For each time point, at least three mice from two different litters were used to characterize the different phenotypes.

For carcinogenesis, mice were treated with DMBA and TPA as previously described³⁰. Briefly, mice from the FVB/N background and from each Cre or CreER line were treated with DMBA at postnatal day 23, 25 and 27 with DMBA (9,10-dimethyl-1,2-benzanthracene) and then treated twice, weekly for several weeks with TPA (12-*O*-tetradecanoyl phorbol-13-acetate). Seven-week-old mice were treated again twice with DMBA. After 25 weeks of treatment, more than 99% of the mice of each genotype develop skin tumours except for the *Nrp1* cKO mice, which fail to develop tumours. After 25 weeks, mice were treated with antibodies or tamoxifen and the size of tumours was followed by direct measurement.

Measurement of tumour growth. Skin tumours were measured using a precision calliper allowing discrimination to size modifications >0.1 mm. Tumour volumes were measured the first day of treatment and every week until the day that they were humanely killed with the formula $V = \pi[d^2 \times D]/6$, where d is the minor tumour axis and D is the major tumour axis.

Histology, immunostaining and imaging. Tissues from FVB/N, CreER and Cre mice were either embedded in OCT and sections were fixed in 4% paraformaldehyde for 10 min at room temperature, or pre-fixed for 2 h in 4% paraformaldehyde and embedded in OCT. Samples were sectioned at 4–6- μ m sections using a CM3050S Leica cryostat (Leica Microsystems).

The following primary antibodies were used: anti-CD34 (rat, 1:100, BD), anti-K5 (rabbit, 1:2,000, Covance), anti- β 4 (rat, 1:200, BD Biosciences), anti-Ki67 (rabbit, 1:200, Abcam), anti-E-cadherin (rat, 1:1,000, Invitrogen), anti-K10 (rabbit, 1:2,000, Covance), anti-endoglin (goat, 1:500, R&D), anti-Nrp1 (goat, 1:100, R&D), anti-VEGFR2 (rat, 1:100, eBioscience), anti-active caspase 3 (rabbit, 1:600, R&D) anti-BrdU (Rat, 1:100, BD), anti-K13 (mouse, 1:100, Abcam), anti-Hmg2 (rabbit, 1:500, Santa Cruz). EdU staining was performed following the manufacturer's instructions (Invitrogen). BrdU or EdU were injected 4 h before mice were humanely killed. Sections were incubated in blocking buffer (PBS/NDS 5%, BSA 1%, Triton 0.2%) for 1 h at room temperature. Primary antibodies were incubated overnight at 4 °C. Sections were rinsed three times in PBS and incubated with secondary antibodies diluted at 1:400 for 1 h at room temperature. The following secondary antibodies were used: anti-rabbit, anti-rat, anti-goat conjugated to Alexa Fluor 488 (Molecular Probes), to rhodamine Red-X (Jackson ImmunoResearch) or to Cy5 (Jackson ImmunoResearch). Nuclei were stained in Hoechst solution (1:1,000) and slides were mounted in DAKO mounting medium supplemented with 2.5% Dabco (Sigma).

Pictures were acquired using Axio Imager M1 Microscope, AxioCamMR3 camera and using Axiovision software (Carl Zeiss).

Isolation of tumour epithelial cells. Tumours from FVB/N mice and mice from each Cre line were digested in collagenase I (Sigma) for 2 h at 37 °C on a rocking plate. Collagenase I activity was blocked by addition of EDTA (5 mM) and then rinsed in PBS supplemented with 2% FCS. After tumour digestion, cells were first incubated in PBS complemented with 30% FCS to block Fc receptors for 15 min at room temperature. Immunostaining was performed using biotin-conjugated anti-CD34 (clone RAM34; BD Pharmingen), FITC-conjugated anti- α 6-integrin (clone GoH3, BD Pharmingen), PE-conjugated anti-CD45 (clone 30F11, eBioscience), PE-conjugated anti-CD31 (clone MEC13.3, BD Pharmingen), PE-conjugated anti-CD140a (clone APA5, eBiosciences), and APC-Cy7-conjugated anti-Epcam (clone G8.8, Biolegend) by incubation for 30 min on ice. A biotin-coupled VEGFR2 antibody (clone avas12a1, eBioscience) was used to determine the expression of VEGFR2 on the different cell populations. Cells were washed and stained using APC-conjugated Streptavidin (BD Pharmingen) for 20 min on ice. Living tumour cells were selected by forward scatter, side scatter and by Hoechst dye exclusion. Fluorescence-activated cell sorting analysis was performed using FACSAria and FACSDiva software (BD Biosciences). Sorted cells were collected either in culture medium for *in vitro* culture experiments or directly in the lysis buffer provided by the manufacturer (Microprep kit, RNAeasy, Stratagene), and RNA extraction was performed according to the manufacturer's protocol. The entire procedure was repeated in at least three biologically independent samples.

Microarray analysis. Total RNA was analysed using mouse whole-genome 430 2.0 array from Affymetrix at the VIB microarray facility. Three different biological samples from CD34⁺ and CD34⁻ TECs were analysed and we compared CD34⁺ to CD34⁻ TECs. The merge of the genes upregulated (>1.5 times) in two among three samples provided a list of 526 genes described in the manuscript as the 'CD34⁺ signature'. The same analysis was performed on CD34⁺ TECs isolated by FACS from *K14CreER:Rosa-VEGF-164* and control mice. The genes

upregulated (>2 times) in *VEGF-164* CD34⁺ TECs compared to control CD34⁺ TECs provided a list of 938 genes (the VEGF signature). The merge of the two comparisons—CD34⁺ signature and VEGF signature—highlighted a list of 122 common genes. Analysis of the microarray was performed by the VIB microarray facility.

Reverse transcription and quantitative PCR (qPCR). Total RNA extraction and DNase treatment of samples were performed using the microprep kit (Stratagene) according to the manufacturer's recommendations. After nanodrop quantification, purified RNA was used to synthesize the first strand cDNA in a 50 μ l final volume, using Superscript II (Invitrogen) and random hexamers (Roche). Control of genomic contaminations was measured for each sample by performing the same procedure with or without reverse transcriptase. qPCR analysis was performed with 4 ng of cDNA reaction as a template, using a Brilliant II Fast SYBR QPCR Master Green mix (Stratagene) and an Agilent technologies Stratagene Mx3500P real-time PCR system. Relative quantitative RNA was normalized using the house-keeping genes β -actin and *Hprt*. Primers were designed using Lasergene 7.2 software (DNASar) and are presented below. Analysis of the results was performed using Mxpro software (Stratagene) and relative quantification was performed using the $\Delta\Delta C_t$ method using β -actin as a reference. The entire procedure was repeated in three biologically independent samples. Error bars represent standard error of the mean (s.e.m.). Results were presented as the fold change over CD34⁻ TECs isolated from the same tumours.

List of primers used. *Vegfr2* mRNA forward 5'-cagtgtactgacagctagaag-3', reverse 5'-acaagcatcagggctgtt-3'; *Vegfa* mRNA forward 5'-aaaaacgaagcgcaagaaa-3', reverse 5'-tttctcgtctgaacaag-3'; *Krt5* (K5) mRNA forward 5'-cagagctgaggacatgcag-3', reverse 5'-cattctcagcctgtgtacg-3'; *Cdh3* mRNA forward 5'-ccttggaggtggaaggaact-3', reverse 5'-tgctcagcaaggtactt-3'; *Cdh1* mRNA forward 5'-cagaatgacaacagccaga-3', reverse 5'-ttcatcagggaggtctctg-3'; *Krt1* mRNA forward 5'-tttgctctctcatcgaca-3', reverse 5'-gtttgggtccgggtgt-3'; *Krt10* mRNA forward 5'-cgtactgtcagggtctggag-3', reverse 5'-gctccagcaggtgttca-3'; *Nrp1* mRNA forward 5'-ccacacacagtggtgtg-3', reverse 5'-ggctcagctgtaggtgctc-3'; *CD34* mRNA forward 5'-gcaccactggtattctctga-3', reverse 5'-ttttctccaacagccatc-3'; *TnC* mRNA forward 5'-gggctatgacaacccagatg-3', reverse 5'-catttaagttccaattcaggtc-3'; *Epha7* mRNA forward 5'-ttaaattgagcgtgtgattg-3', reverse 5'-tcaaacgaccactgcaaac-3'; *Aen* mRNA forward 5'-acgtgaaactgggaaagc-3', reverse 5'-agccagctcagaggttg-3'; *Ank3* mRNA forward 5'-cgaatgcaacagcagcaataa-3', reverse 5'-ccactctcactcgttctt-3'; *Anln* mRNA forward 5'-acaatcaagga caaactgc-3', reverse 5'-gcgtccaggaagcgtta-3'; *Ano1* mRNA forward 5'-accaagccaaagtacagat-3', reverse 5'-tgcagctgagtagtaccgcatc-3'; *Anxa3* mRNA forward 5'-aggctgatcttcacctcg-3', reverse 5'-aagccgagatcacagcaatc-3'; *Atp10d* mRNA forward 5'-gaggtggtgaaattggtctg-3', reverse 5'-atcattggcaccgtcacc-3'; *Cadm4* mRNA forward 5'-tgtctgtcacaggaacc-3', reverse 5'-caggccagtagcgtgag-3'; *Camk1d* mRNA forward 5'-ctctactggtcagcaact-3', reverse 5'-ctgtgtaaaccccttcca-3'; *Ccna2* mRNA forward 5'-cttgctgaccacaagcaataa-3', reverse 5'-caaacctagttctcccaaaa-3'; *Ccnd1* mRNA forward 5'-gagattgtgccatc-3', reverse 5'-ctctcttctgcatctctgct-3'; *Ccng1* mRNA forward 5'-tggcagattctgtaataaagag-3', reverse 5'-cagtgaggacattcttctc-3'; *CD133* mRNA forward 5'-gaaggagccagccttagagg-3', reverse 5'-ggtcattcactcaaaagtaccatc-3'; *Cdc14b* mRNA forward 5'-acttggcggcctgaaag-3', reverse 5'-tcagcacagctaggagacat-3'; *Krt13* (K13) mRNA forward 5'-agtcccagctgagcatgaa-3', reverse 5'-gatgagcccttgatctgt-3'; *Cdc5l* mRNA forward 5'-aacgcagtgaggaccat-3', reverse 5'-gtcccttggcaggtttg-3'; *Cdkn2a* mRNA forward 5'-gggtttctgtgtgactgtc-3', reverse 5'-ttgcccactcatcactc-3'; *Cep55* mRNA forward 5'-tttcggctctgtaactg-3', reverse 5'-tctggaactcactcactgtaactg-3'; *Cldn4* mRNA forward 5'-gaggctggggaccta-3', reverse 5'-gcaagacagtcgggaaag-3'; *Crabp2* mRNA forward 5'-tgaggaaatgtaaaagctctg-3', reverse 5'-tctctgttctgactgactgct-3'; *Cyp4f39* mRNA forward 5'-aaagaagaagcagaagaa-3', reverse 5'-tgcacaggtagctggtgag-3'; *Ddit4l* mRNA forward 5'-ctggtgtctccccacac-3', reverse 5'-tctactcagtaagggacac-3'; *Dmrt2* mRNA forward 5'-agtcttggctcgggttgc-3', reverse 5'-ttctgcaattggcctctg-3'; *Ecm1* mRNA forward 5'-tccagagcagcctgatctt-3', reverse 5'-atctctcgtggtgtaagc-3'; *Eomes* mRNA forward 5'-accggcaccacagcaga-3', reverse 5'-aagctcaagaaggaacatgc-3'; *Ephx3* mRNA forward 5'-tcccctgactgatccag-3', reverse 5'-tggaaagtcagacatagacaacagc-3'; *Esm1* mRNA forward 5'-cagatgacagcagcaaac-3', reverse 5'-gatgctgagtcacagctctg-3'; *Exoc4* mRNA forward 5'-tgaccaacatcaccatgca-3', reverse 5'-gctgtgtgtacacatcctg-3'; *Fads2* mRNA forward 5'-attcgggagaagatgctacg-3', reverse 5'-aagaactgcccagcaagtc-3'; *Fam129a* mRNA forward 5'-tacggctcagggaaatgac-3', reverse 5'-gctcctcaccagcctta-3'; *Far1* mRNA forward 5'-cactgtgctgactgtaaga-3', reverse 5'-agctgtctgtgactatc acattt-3'; *Gpx2* mRNA forward 5'-gttctgctccctcctg-3', reverse 5'-tccagatctcctgttctga-3'; *Grlh3* mRNA forward 5'-aaggaagatgcaaatgactg-3', reverse 5'-tctctctacttagtaggaaa-3'; *Gsta1* mRNA forward 5'-cttctgacccttccctc-3', reverse 5'-gctgcccagctgtaggaac-3'; *Gsta2* mRNA forward 5'-cagagtcgggaagattgga-3', reverse 5'-agaatgctgctgctgacac-3'; *Hmg2* mRNA forward 5'-aaggc

agcaaaaacaagagc-3', reverse 5'-ccgtttttcctaagtgtc-3'; *Igf2bp2* mRNA forward 5'-gggaaatcatggaagtgtgacta-3', reverse 5'-cgggatgtccgaatctg-3'; *Kcmn4* mRNA forward 5'-tctgcacgctgagatgtgt-3', reverse 5'-accaggagcaggtacagcac-3'; *Krt18* mRNA forward 5'-agatgacaccaatcacaagg-3', reverse 5'-tccagacttgacttctc-3'; *Krt42* mRNA forward 5'-tgcagatcgagagcctga-3', reverse 5'-acgaaggcattcattcc-3'; *Lrrfip1* mRNA forward 5'-gtttgccgaagtgaagagg-3', reverse 5'-aatttaggattatccatgtttctcg-3'; *Neto2* mRNA forward 5'-tccaccaacaaggagtgtatct-3', reverse 5'-agcgttcatcaaaaggtcagc-3'; *Nrp2* mRNA forward 5'-atggctggacaccaat-3', reverse 5'-atggtaggaagcagcaggt-3'; *Phlda2* mRNA forward 5'-tcagcgtctgagtctgaaa-3', reverse 5'-tgggctctgtctgatgc-3'; *Prkg2* mRNA forward 5'-ttggcaaaagcaggt-3', reverse 5'-tcaactgtggctgatcag-3'; *Ptpr1* mRNA forward 5'-gactgagctccacccttaa-3', reverse 5'-gtaaggatccacagaggaaca-3'; *Ptpr2* mRNA forward 5'-ggcactcaggagtccaaca-3', reverse 5'-gaccaatcagagactcagccta-3'; *Rapgef3* mRNA forward 5'-ggatcaattctgcccgtgt-3', reverse 5'-gttgagccccagggatg-3'; *Sox2* mRNA forward 5'-tccaaaactaacaacaatcg-3', reverse 5'-gaagtcgaatgggagaaaa-3'; *Spp1* mRNA forward 5'-ggagaaaccagcaag-3', reverse 5'-tgccagaatcagcactttcac-3'; *Krt14* mRNA forward 5'-atcgaggactgaagagcaa-3', reverse 5'-tcgatctgaggagcatt-3'; *CD45* mRNA forward 5'-aatggctctcagagaccacata-3', reverse 5'-agtcaggctgtgggaca-3'; *CD31* mRNA forward 5'-cggtgttcagcagatcc-3', reverse 5'-cgacaggatgaaatcaca-3'; *pdgfra* mRNA forward 5'-gtcgttgactcagtgga-3', reverse 5'-ccagcatggtgatacctttgt-3'; *CD11b* mRNA forward 5'-aagatgctgggaggtc-3', reverse 5'-gtcataagtgacagctctgga-3'; *vim* mRNA forward 5'-ccaacctttctccctgaa-3', reverse 5'-tgatgggtgcaaccagag-3'; *tek (tie2)* mRNA forward 5'-cataggagaaactgttacc-3', reverse 5'-cccacttctgagctcacatc-3'.

Culture of tumour epithelial cells. 3T3 feeder cells were γ -irradiated and plated on 12-well plates. The next day, sorted CD34⁺ and CD34⁻ epithelial tumour cells were plated on wells pre-cultured with 3T3 feeders cells in keratinocyte medium (MEM medium supplemented with 15% FBS, 0.4 $\mu\text{g ml}^{-1}$ hydrocortisone, 5 $\mu\text{g ml}^{-1}$ insulin, 10 ng ml^{-1} EGF, 2×10^{-9} M T3, 1% penicillin/streptomycin, 2 mM L-glutamine). Twenty-four hours later, the cells were left untreated (control) or treated with VEGF (50 ng ml^{-1} , R&D), anti-VEGF-A (20 $\mu\text{g ml}^{-1}$, R&D) or anti-Nrp1 blocking antibodies (10 $\mu\text{g ml}^{-1}$, Genentech). We used two distinct Nrp1-blocking antibodies: anti-Nrp1a, which blocks binding of semaphorins, and anti-Nrp1b, which blocks binding of VEGF-A. The medium was changed every other day for at least 1 week. At the end of the treatment, the feeders were blasted using PBS + EDTA (1 mM). The keratinocytes were trypsinized and counted. For induction of differentiation, untreated CD34⁺ clones were cultured overnight in keratinocyte medium supplemented with only 2% of serum after blasting of the feeder cells. The next day, the cells were cultured in 2% serum medium for 48 h with 1.7 mM Ca²⁺ to induce differentiation or kept in a low Ca²⁺ medium

(0.07 mM). The keratinocytes were then trypsinized and RNA extraction was performed as described above.

ELISA for VEGF-A. Control and *K14CreER:Rosa26-VEGF-164* mice were killed 1 week after tamoxifen injection (15 mg per week) and tumours were excised and weighted before being dissociated mechanically at 4 °C in PBS supplemented with a cocktail of protease inhibitors (Roche Diagnostics). Tumour lysates were centrifuged at 13,000 r.p.m. min⁻¹ for 5 min and VEGF-A concentration was assessed in the supernatant by ELISA (R&D Systems) following the manufacturer's recommendations.

Secondary tumour assays. CD34⁺ TECs were isolated by FACS from control, *K14CreER:Rosa26-VEGF-164* and *K14CreER:VEGF^{fl/fl}* mice 1 week after tamoxifen injection (15 mg per week). Cells were harvested in 4 °C medium supplemented with 20% serum and 1% penicillin/streptomycin. Cells were then washed in PBS complemented with 1% penicillin/streptomycin and re-suspended in matrigel (Sigma). 1,000 CD34⁺ TECs re-suspended in 50 μl of matrigel were injected subcutaneously to Nude mice (Charles River). Three injections per mouse were performed. Secondary tumours were detected by palpation and mice were killed 3 weeks after grafting when tumours reached 50 mm³ to perform immunostainings.

Symmetry of cell division. To determine the plane of cell division, we performed co-immunostaining for $\beta 4$ integrin, which marks the basal lamina, and NuMA (Novus), which marks the pair of centrosomes at the opposite side of cells in late prophase/metaphase. Measurement of the angle formed by the basal lamina and the centrosomes allows us to determine whether mitoses are symmetric (0–40°) or asymmetric (50–90°). Angles between 40° and 50° have been counted and classified as 'undetermined' to limit false-positive results.

Statistics. Data represent mean \pm s.e.m. Statistical significance was calculated by Student's *t*-test, ANOVA or Fisher's exact test where indicated (Origin 7.0), considering $P < 0.05$ as statistically significant.

26. Vasioukhin, V., Bauer, C., Degenstein, L., Wise, B. & Fuchs, E. Hyperproliferation and defects in epithelial polarity upon conditional ablation of alpha-catenin in skin. *Cell* **104**, 605–617 (2001).
27. Vasioukhin, V., Degenstein, L., Wise, B. & Fuchs, E. The magical touch: genome targeting in epidermal stem cells induced by tamoxifen application to mouse skin. *Proc. Natl Acad. Sci. USA* **96**, 8551–8556 (1999).
28. Gerber, H. P. et al. VEGF is required for growth and survival in neonatal mice. *Development* **126**, 1149–1159 (1999).
29. Gu, C. et al. Neuropilin-1 conveys semaphorin and VEGF signaling during neural and cardiovascular development. *Dev. Cell* **5**, 45–57 (2003).
30. Abel, E. L., Angel, J. M., Kiguchi, K. & DiGiovanni, J. Multi-stage chemical carcinogenesis in mouse skin: fundamentals and applications. *Nature Protocols* **4**, 1350–1362 (2009).